

Original Article

Effect of stellate ganglion ischaemia on vertebral artery remodelling after bilateral common carotid artery ligation: an experimental study

Adem Yilmaz¹, Osman Tanriverdi¹, Ilhan Yilmaz¹, Kamran Urgan¹, Ahmet Murat Musluman¹, Muhammet Calik², Mehmet Dumlu Aydin³

¹Department of Neurosurgery, Şişli Hamidiye Etfal Research and Education Hospital, Istanbul, Turkey; Departments of ²Pathology, ³Neurosurgery, School of Medicine, Atatürk University, Erzurum, Turkey

Received January 13, 2016; Accepted May 19, 2016; Epub November 15, 2017; Published November 30, 2017

Abstract: To determine whether a relationship exists between the density of degenerated neurons in the stellate ganglion and the severity of dilatation of vertebral arteries (VAs) after bilateral common carotid artery ligation (BCCAL). This study was conducted on 25 rabbits, which were divided into 3 groups: baseline control group (n = 5), sham group without ligation (n = 5), and the BCCAL group (n = 15). Common carotid arteries (CCA) were exposed bilaterally, proximal to the level of bifurcation. After two months, VAs and stellate ganglions were examined histopathologically. The VA vasodilatation index (VDI) and degenerated neurons density (DND) values of the stellate ganglions were estimated stereologically. The results were analysed statistically using the Mann-Whitney U test. The mean VA length and mean VDI value in control animals was 11.30 ± 1.60 mm and 2.30 ± 0.91 , respectively. The controls' mean neuron density of stellate ganglions was around $11.200 \pm 1.240/\text{mm}^3$, and mean DND was $27 \pm 9/\text{mm}^3$ ($P > 0.5$). The mean VA VDI value in the sham group was 1.60 ± 0.59 , and the DND of the stellate ganglions was approximately $960 \pm 170/\text{mm}^3$ ($P < 0.005$). Six animals developed severe vasodilatation ($\text{VDI} < 1.50$), in which the mean VDI value of the VAs was around 1.04 ± 0.13 , and the DND of stellate ganglions was $3.130 \pm 930/\text{mm}^3$ ($P < 0.0005$). In contrast, the mean VA VDI value in animals in which slight vasodilatation occurred was estimated as 1.89 ± 0.11 , and the DND of the stellate ganglions was $452 \pm 110/\text{mm}^3$ (n = 9) ($P < 0.001$). Hypertrophic VAs were observed in these animals. Stellate ganglion ischaemia after BCCAL may be beneficial in reducing craniocerebral blood flow via ischaemic blockade.

Keywords: Carotid artery, ischaemia, ligation, stellate ganglion, vertebral artery

Introduction

BCCAL causes a major redistribution of blood flow to the head with increased flow through the vertebral and basilar arteries. Important morphologic and histopathologic changes occur in the craniocervical vessels after this procedure. Increased intraluminal pressure and retrograde blood flow in the posterior arteries result in vascular remodelling and trophic changes in the major cerebral arteries [1]. BCCAL induces aneurysm formation and remodelling [2, 3]. Dilatation, tortuosity, and fusiform or lateral wall aneurysms are observed at non-branching sites of basilar arteries [4]. In one study, all animals that underwent CCA ligation developed nascent aneurysm formation char-

acterized by a bulge with thinned media and no internal elastic lamina near the basilar terminus [5]. The blood supply to the stellate ganglion is maintained by the external carotid artery and other portions of the deep cervical branches of the subclavian artery [6]. Although BCCAL can cause stellate ganglion ischaemia, we were surprised to find that retrograde blood flow was able to protect the carotid bodies from this ischaemic insult and that the protected carotid bodies maintained cerebral circulation within normal limits [7].

Cerebral vascular innervation is maintained by various autonomic nerve fibres, as well as through humoral and chemical factors. The net effect of parasympathetic cranial nerves is

Stellate ganglion functions on vertebral arteries

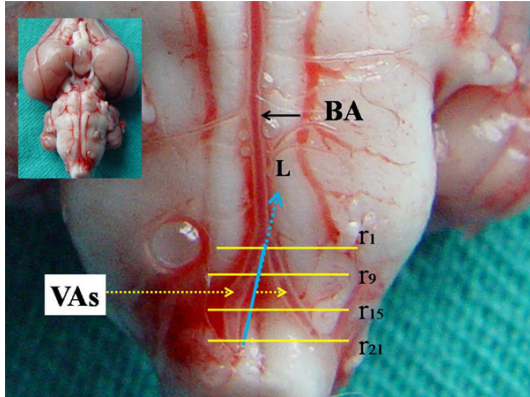


Figure 1. Gross appearance of brain together with basilar artery (BA), vertebral arteries (VAs), and volume estimation methods with their radius values at consecutive 20 radius (r_{1-21}) and lengths (L).

vasodilatory, and the sympathetic output of the stellate ganglions has vasospastic effects on cerebral arteries [8-10]. Sympathetic innervation of the VAs is maintained by cervical sympathetics [11]. Additionally, trigeminal nerve endings provide dense and vasodilatory innervation of cerebral vessels [8]. This innervation regulates the VAs and their function by altering the lumen diameter, permeability, and secretory ability. These nerves play an important role in the determination of basilar artery morphology after BCCAL. A rabbit model was developed to examine the effects of bilateral common carotid ligation on stellate ganglion neuron density and on volumetric changes in the basilar arteries. Two months after BCCAL, changes in the VAs were assessed histologically within all portions of the VAs. For evaluating the degree of vasospasm, the VDI values of the VAs were measured with respect to the lumen radius. The Cavalieri and stereologic methods were used to estimate the VDI changes in the VAs that were secondary to vasospasm [12, 13]. Additionally, neurodegenerative changes in stellate ganglions were detected due to decreased blood flow after BCCAL. The high neuronal density of the stellate ganglion may have a preventive effect on basilar artery elongation, enlargement, vascular intimal ruptures and de novo aneurysm formation.

Materials and methods

This study was performed on 25 anaesthetized adult male New Zealand rabbits (3.7 ± 0.4 kg). The animal protocols were approved by the

Ethics Committee of Atatürk University, Medical Faculty. Animal care and the experiments were performed according to the guidelines set forth by the same ethics committee. The animals were randomly divided into three groups: baseline group ($n = 5$), sham group ($n = 5$) and BCCAL group ($n = 15$). A balanced, injectable anaesthetic was used to reduce pain and mortality. After inducing anaesthesia with isoflurane by face mask, 0.2 mL/kg of the anaesthetic combination (ketamine HCL, 150 mg/1.5 mL; xylazine HCL, 30 mg/1.5 mL; and distilled water, 1 mL) was subcutaneously injected prior to surgery. During the procedure, a dose of 0.1 mL/kg of the anaesthetic combination was used when required. All animals were placed in the supine position and secured to the operation table. The anterior cervical regions were prepared for the application of BCCAL. After a 3 cm mid-cervical median incision, the bundle of CCA-vagal nerve-jugular vein-sympathetic chain was found bilaterally in all 20 animals. Then, CCAs were dissected gently from their associated tissues and structures. BCCAL was performed on 15 animals (Study Group; $n = 15$), while the remainder received no intervention (sham Group; $n = 5$). The animals were followed for 2 months without any additional medical treatments prior to euthanasia. All brains and stellate ganglions were extracted for histologic examination. These structures were fixed in 10% formalin solution for 7 days. Then, 5 μ m tissue sections were taken from the VAs at the mid-pontine level. All specimens were stained with haematoxylin & eosin (H&E), and the stellate ganglions were also stained by terminal deoxynucleotidyl transferase dUTP nick-end labelling (TUNEL).

For the calculation of the VA VDI, all VAs were considered as cylinders, in light of their morphological characteristics, and simple geometric formulas were used to estimate surface area. As a measure of the degree of vasospasm, the use of the VA VDI was preferred over sole measurement of the lumen radius because the volume estimation method can be readily performed and is intuitively simple, more reliable, free from assumptions regarding the vessel diameter at various segments and unaffected by overestimation error of the radius. VAs of all animals were cut at a 20 segment distance from the point at which the internal carotid arteries arise to the entrance of the posterior cerebral arteries. Next, 20 histopathological

Stellate ganglion functions on vertebral arteries

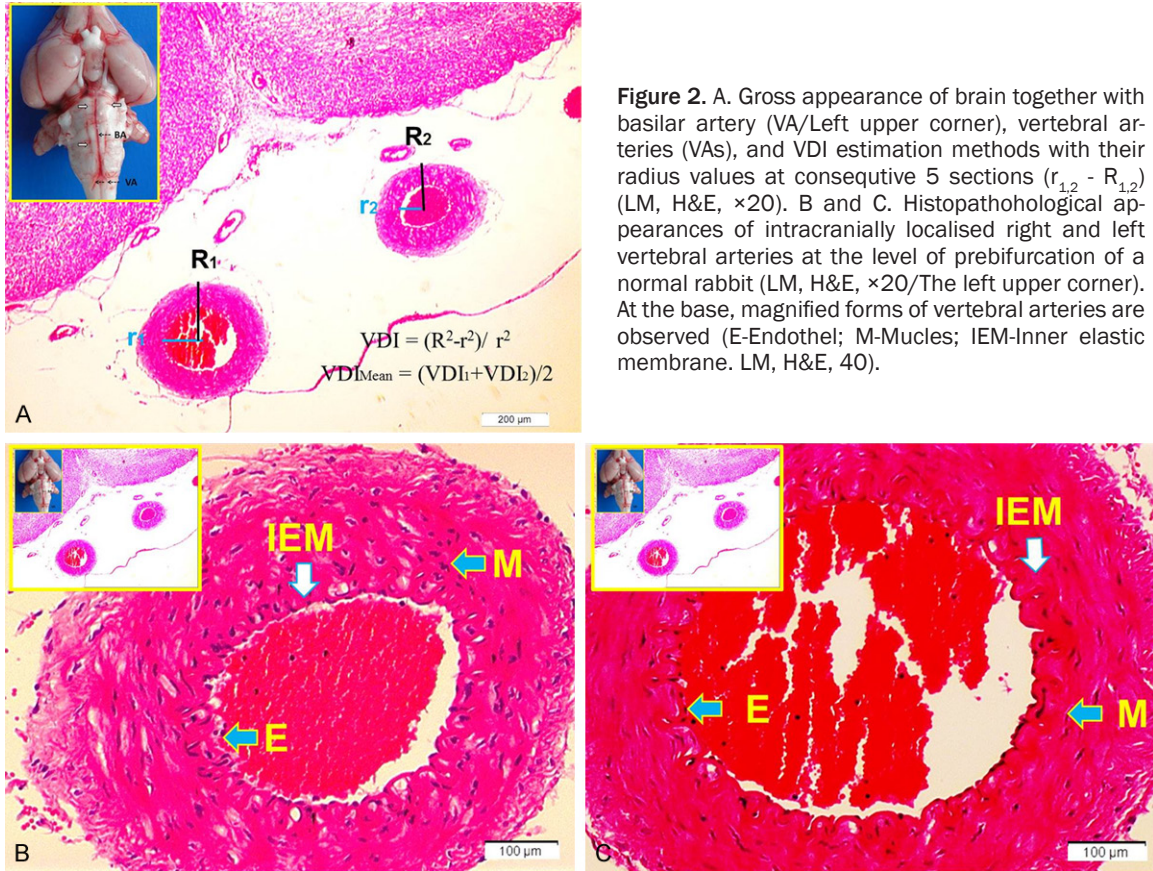


Figure 2. A. Gross appearance of brain together with basilar artery (VA/Left upper corner), vertebral arteries (VAs), and VDI estimation methods with their radius values at consecutive 5 sections ($r_{1,2} - R_{1,2}$) (LM, H&E, $\times 20$). B and C. Histopathological appearances of intracranially localised right and left vertebral arteries at the level of prebifurcation of a normal rabbit (LM, H&E, $\times 20$ /The left upper corner). At the base, magnified forms of vertebral arteries are observed (E-Endothel; M-Mucous; IEM-Inner elastic membrane. LM, H&E, 40).

sections at 5 μm intervals were obtained by microtome for each designation and are represented by lines 1 through 21. To prevent any confusion, these numbers were changed to letter designations (a-t) in all formulas. The mean external and internal (luminal) diameters of each section were measured, with the external radius represented as R_1 and the internal radius represented as r_1 . The mean radius value of each VA was calculated as $R \text{ mean} = (R_a + R_b + R_c + \dots R_t)/21$, and the mean lumen radii were calculated as $r \text{ mean} = (r_a + r_b + r_c + \dots r_t)/21$. The wall ring surface values were calculated from the following formula: $S_1 = \pi R_M^2 - \pi r_m^2$. The lumen surface area was calculated with the same method using the following formula: $(S_2) = \pi r_m^2$. For both formulas, R_M is the external radius and r_m is the internal (lumen) radius. The VDI was calculated as a proportion of S_1/S_2 . $\text{VDI} = S_1/S_2 = (\pi R_M^2 - \pi r_m^2)/\pi r_m^2 = \pi (R_M^2 - r_m^2)/r_m^2 = (R_M^2 - r_m^2)/r_m^2$. In summary, $\text{VDI} = (R^2 - r^2)/r^2$.

Stellate ganglions were extracted bilaterally to estimate neuron density. Then, they were horizontally embedded in paraffin blocks to observe all roots during histopathological examination.

The physical dissector method was used to evaluate the number of neurons in the stellate ganglion. Two consecutive sections (dissector pairs) obtained from reference tissue samples were mounted on each slide. The paired reference sections were reversed to double the number of dissector pairs without the need to cut new sections. The mean numerical density of normal and degenerated neurons in the stellate ganglion (N_V/G_V) per mm^3 was estimated using the following formula:

$$N_V/G_V = \Sigma Q/\Sigma Axd$$

in which $\Sigma Q \cdot N$ is the total number of counted neurons appearing only in the reference sections, d is the section thickness, and A is the area of the frame counted. The most effective way of estimating ΣA for the set of dissectors is via $\Sigma A = \Sigma P \cdot a$. ΣP is the total number of counted points in a set frame, and a is a constant area associated set point. **Figure 4A** and **4B** shows the area of counting frames. The Cavalieri volume estimation method was used to obtain the total number of neurons in each specimen. The total number of neurons was

Stellate ganglion functions on vertebral arteries

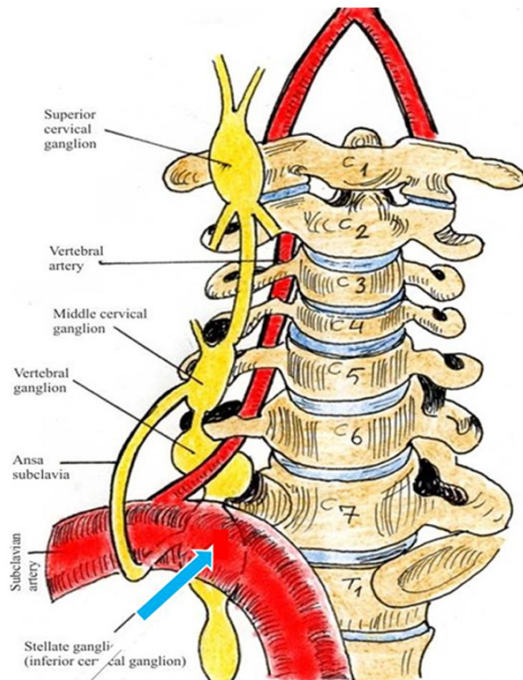


Figure 3. A schematic representation of stellate ganglion and related anatomical structures.

calculated by multiplication of the volume (mm^3) and the numerical density of neurons in each stellate ganglion. The numbers of both normal and degenerated neurons in the stellate ganglions from each animal were counted to analyse if there is any relationship between the ischemic neurodegeneration of stellate ganglions and VDI values of vertebral arteries.

The differences between the VDI values of the vertebral arteries and neuron densities of the stellate ganglia were compared statistically. The data analysis were evaluated by the Mann-Whitney *U*-test. Differences were considered to be significant at $P < 0.05$.

Results

Three of the animals in the BCCAL group ($n = 3$) died within the first week, while the remainder ($n = 12$) were observed for two months. Clinically, ischaemic attacks, unconsciousness, convulsions, cardiac arrhythmias and breathing difficulty were frequently observed in the three animals that died.

Anatomopathological examination of the brains showed that all VAs localized to the anterior surface of the bulbous and extended from the

margin of the foramen magnum to the fusion point of VAs (**Figure 1**). The lengths of the VAs were 19.50 ± 1.20 mm. Vertebral arteries convolutions were more prominent in the animals with induced BCCAL than in the sham and control groups. The histopathological examination results of the normal VAs, including the lumen diameter, inner elastic membrane (IEM) convolution, endothelial cell structure, vascular wall muscles and adventitia are presented in **Figure 2A-C**. Schematic representation of stellate ganglions and their anatomical localizations are depicted in **Figure 3**. The histological appearance of the stellate ganglions and the neuron density estimation method are presented in **Figure 4A** and **4B**. TUNEL staining detected apoptotic neurons (**Figure 5**). In the histopathological examination of VAs in the sham group, minimal IEM flattening, greater luminal surface and VA expansion, wall thinning and increased VDI values of VA were observed (**Figure 6A** and **6B**). In the BCCAL group, leptomeningeal thickening as well as VA elongation and convolution were macroscopically observed in the animals with less neuron degeneration (**Figure 7A** and **7B**). In the animals that showed more degenerated neurons in stellate ganglions, IEM flattening, intimal thinning, endothelial cell shrinkage, desquamation and endothelial cell loss, luminal enlargement, dilatation, endothelial microthrombus and even wall rupture were observed (**Figure 8A** and **8B**). In stereological examination of VAs and stellate ganglions, the following results were found. In control animals, the mean VA length was 11.30 ± 1.60 mm, and the mean VDI value was 2.30 ± 0.91 . In the same group, the mean neuron density of stellate ganglions was estimated to be $11.200 \pm 1.240/\text{mm}^3$, and the mean DND was $27 \pm 9/\text{mm}^3$ ($P > 0.5$). In the sham group, the mean VDI value of the VAs was 1.60 ± 0.59 , and the DND of the stellate ganglions was estimated to be $960 \pm 170/\text{mm}^3$ ($n = 5$) ($P < 0.005$). In animals that developed severe vasodilatation ($\text{VDI} < 1.50$), the mean VDI value of the VAs was estimated to be 1.04 ± 0.13 , and the DND of the stellate ganglions was $3.130 \pm 930/\text{mm}^3$ ($n = 6$) ($P < 0.0005$). In contrast, for animals that developed slight vasodilatation, the mean VDI value of the VAs was estimated to be 1.89 ± 0.11 , and the DND of the stellate ganglions was $452 \pm 110/\text{mm}^3$ ($n = 9$) ($P < 0.001$). Interestingly, hypertrophic VAs were noticed in these animals.

Stellate ganglion functions on vertebral arteries

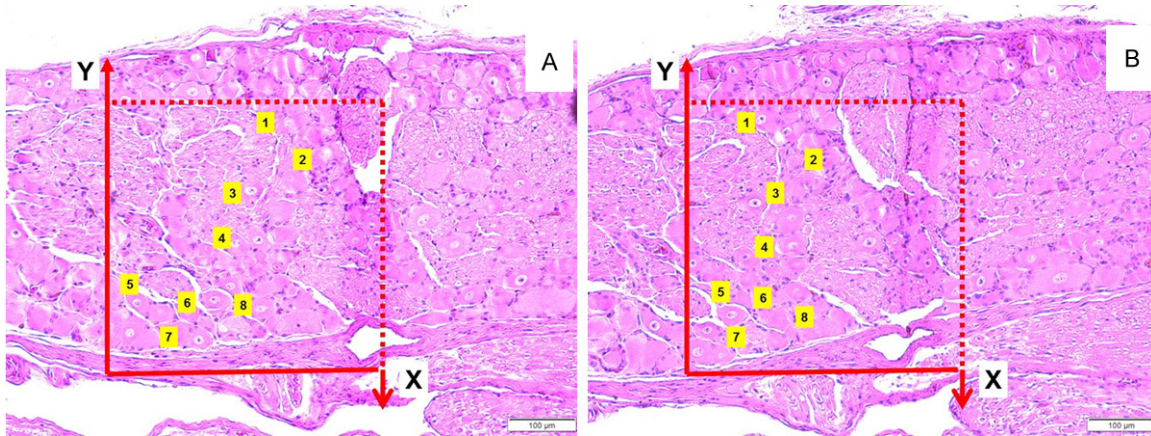


Figure 4. (A and B) Stereological histopathological demonstration of stellate ganglion at the C8 level. Stereologic cell counting method of stellate ganglion is seen in a rabbit. Application of the physical dissector method in which micrographs in same fields of view (A, B) are taken from two parallel adjacent thin sections separated by a distance of 5 μm . Upper and right lines of unbiased counting frames represent the inclusion lines and the lower and left lines including the extensions are exclusion lines. Any neuron nucleolus hitting the inclusion lines is excluded and nucleolus profiles hitting the inclusion lines and located inside the frame are counted as dissector particles unless their profile extends up to the look-up section. The number of neurons from the two dissectors occurs in a volume given by the product of the counting frame area and distance between the sections. The numerical density of neurons is calculated from $N_VGN = \sum Q^- GN / t \times A$. In this application, the nucleoli of normal neurons marked with '1 and 5' are dissector particles on A section as it disappeared section B, and the marked with 2, 3, 5-7 are dissector particles and 1, 4, 8 are not dissector particles. The nucleoli appears in both sections don't accept as dissector particles. The degenerated neurons (DN) are estimated the same method of normal neurons (H&E, 20, LM). Anatomical representation of stellate ganglion is seen at the right sides of the pictures.

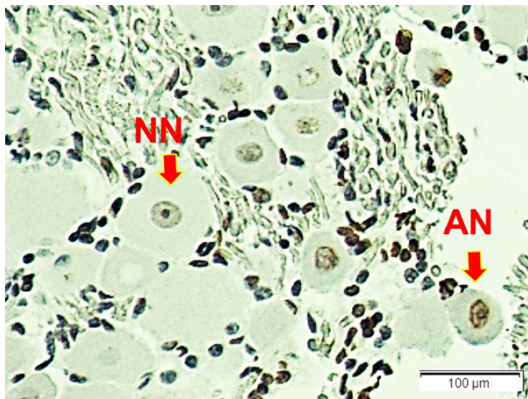


Figure 5. Histopathological appearance of stellate ganglion belong to a rabbit of study group. Normal (NN) and apoptotic (AN) neurons are seen (LM, Tunnel stain).

In the statistical analysis, the mean neuron density of stellate ganglia have its lowest levels in animals that developed severe artery dilatation, and this difference was significant ($P < 0.001$). The mean neuron density of stellate ganglia was found to be highest in animals that developed less severe vertebral artery dilatation, a finding that was also significant ($P < 0.05$). There were no important differences between the control and sham groups ($P > 0.05$).

We importantly informed that BCCAL related ischemic neurodegeneration of stellate ganglia were meaningful contribution on the vertebral arteries dilatation ($P < 0.0001$).

Discussion

BCCAL causes major redistribution of blood flow to the head, with increased and retrograde blood flow through the vertebral and basilar arteries. Important morphologic and histopathologic changes occur in the vertebral, basilar, posterior communicating, and posterior cerebral arteries within four months, and intracranial vascular changes largely return to normal after four months. Here, we discuss a mechanism that could explain these trophic vessel changes in response to increased blood flow as well as explore a possible correlation between these findings and several brain vascular diseases [1]. Haemodynamic insult by BCCAL has been shown to induce aneurysmal remodelling at the basilar terminus in a rabbit model. In these rabbits, aneurysmal remodelling begins when local haemodynamic forces exceed specific limits at the basilar terminus. Dangerous haemodynamic changes are likely to induce aneurysmal remodelling [2]. BCCAL causes the

Stellate ganglion functions on vertebral arteries

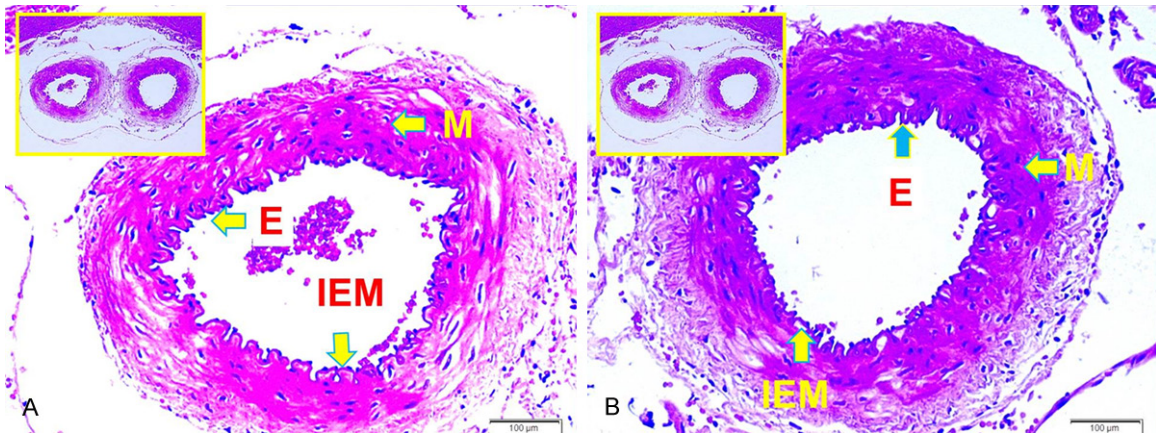


Figure 6. A and B. Histopathological appearances of intracranially localised right and left vertebral arteries at the level of prebifurcation of a rabbit after two months of BCCAL SHAM (LM, H&E, $\times 20$ /The left upper corner). At the base, magnified forms of hyperthrophic vertebral arteries are observed (E-Endothel; M-Mucles; IEM-Inner elastic membrane. LM, H&E, $\times 40$).

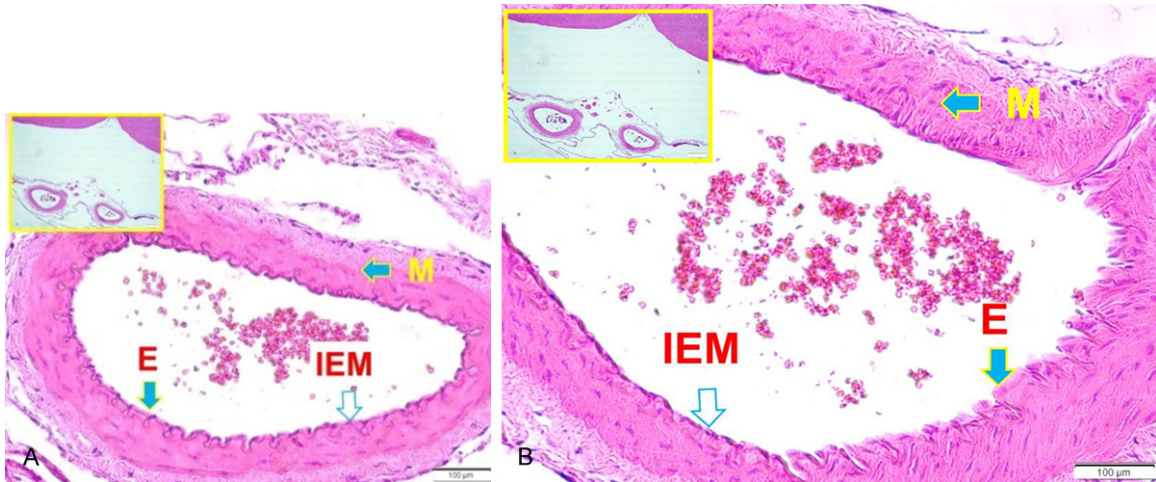


Figure 7. A and B. Histopathological appearances of intracranially localised right and left vertebral arteries at the level of prebifurcation of a rabbit after two months of not applied BCCAL and only SHAM (LM, H&E, $\times 20$ /The left upper corner). At the base, magnified forms of slightly dilated vertebral arteries are observed (E-Endothel; M-Mucles; IEM-Inner elastic membrane. LM, H&E, $\times 40$).

development of arteriovenous malformation and mental changes [14]. In one study, vascular corrosion casts of the cerebral arteries were examined by scanning electron microscopy three months after BCCAL. Forty-eight arterial changes including dilatation, tortuosity, and fusiform or lateral wall aneurysms were observed at non-branching sites [4]. After BCCAL, hemodynamic insults at arterial bifurcations are hypothesized to play a key role in intracranial aneurysm formation. Unilateral or BCCAL produces varying degrees of increase in compensatory basilar artery flow. All CCA-ligated rabbits showed nascent aneurysm formation char-

acterized by a bulge with thinned media and without internal elastic lamina near the basilar terminus [5]. Pialmicrovessel alterations due to transient bilateral CCA occlusion also occurred [15]. BCCAL relies on basilar blood flow and basilar enlargement [16]. It causes increased intraluminal pressure, basal lamina destruction, endothelial injury and acute vessel dilatation in brain micro vessels. The blood brain barrier also gets destroyed [17]. BCCAL causes retrograde blood flow and protects many tissues supplied by carotid arteries such as the cingulum bundle [7]. BCCAL may lead to Pcom aneurysms, which cause cerebral vascular

Stellate ganglion functions on vertebral arteries

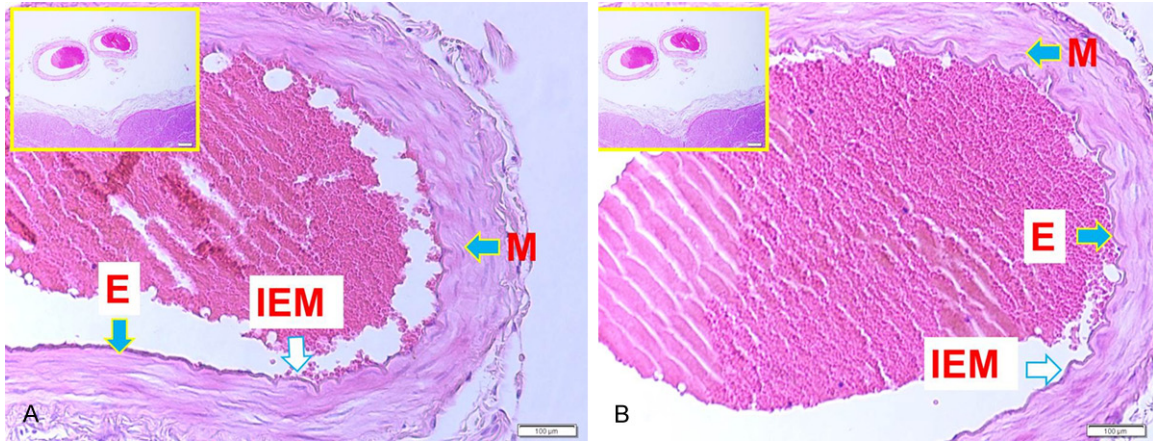


Figure 8. A and B. Histopathological appearances of intracranially localised right and left vertebral arteries at the level of prebifurcation of a rabbit after two months of BCCAL with important stellate ganglion ischemia detected animals (LM, H&E, $\times 20$ /The left upper corner). At the base, magnified forms of dilated vertebral arteries are observed (E-Endothel; M-Mucles; IEM-Inner elastic membrane. LM, H&E, $\times 40$).

innervation problems by compressing the oculomotor nerves. It also leads to basilar artery ectasia or can cause autonomic dysfunction by compressing the lower cranial parasympathetic nerves [1, 3]. Because the blood supply of the stellate ganglion is maintained by the external carotid artery and other parts of the deep cervical branches of the subclavian artery, BCCAL can reduce blood flow and cause neurodegeneration in stellate ganglions. Neurodegenerative changes in ganglions can reduce sympathetic neurotransmitters, which affect VAs and prevent vasospastic changes from occurring [6]. This neurophysiologic mechanism of vasospasm prevention may be useful for the maintenance of cerebral blood flow immediately after BCCAL. It may subsequently lead to dangerous effects such as dolichoectasia, vascular rupture and aneurysm formation in the posterior circulation arteries at later times.

Cerebral vascular innervation is maintained by various autonomic nerve fibres and neurochemical networks that contribute to the control of brain vessel diameter and blood flow. The vasodilatory parasympathetic output to the brain consists of postganglionic fibres of the ciliary ganglion of the third cranial nerve, the sphenopalatine ganglion of the seventh cranial nerve and the otic ganglion of the ninth cranial nerve [8-10]. The vasospastic sympathetic innervation of cerebral vessels originates from the postganglionic fibres of the superior sympathetic ganglion and its largest efferent branch, the carotid nerve, which is a component of the

carotid plexus [18]. The sympathetic system plays an important role in the pathogenesis of vasospasm in subarachnoid haemorrhage [9]. Sympathetic innervation of VAs is maintained by cervical sympathetics [11]. Bilateral cervical ganglionectomy results in significant vasodilatation in the basilar artery within one month [19]. However, certain studies have found that sympathectomy prevents basilar artery vasospasm in subarachnoid haemorrhage [20]. The large cerebral arteries, venous sinuses and dura mater are pain-sensitive and are innervated primarily by branches of the ophthalmic division of the trigeminal nerve [21]. Trigeminal nerve endings originating from the trigeminal ganglion provide dense vasodilatory innervation of major cerebral vessels [22]. Ablative lesions in the trigeminal ganglion prevent basilar artery dilation [23]. However, pre-ganglionic lesions do not affect the baseline diameter [21]. Additionally, it is well-known that the trigeminal nerve endings have vasodilatory effects on basilar arteries [22]. Stereological methods have been used to estimate the neuron density and basilar artery volume [12, 13]. The severity of basilar artery vasospasm was higher in rabbits with increased neuron density in the stellate ganglion.

Cervical sympathectomy prevents acute vasospasm induced by meningeal haemorrhage in rabbits [24]. Sympathetic nerves also influence cytoskeletal protein remodelling through phenotypic modulation in vascular pathologies such as atherosclerosis [25]. Cervical spinal

Stellate ganglion functions on vertebral arteries

cord stimulation is able to prevent “early spasm” due to subarachnoid haemorrhage in all animals [26, 27]. The results of one study suggest that elimination of sympathetic nervous system activity in rabbits prevents vasospasm upon subarachnoid haemorrhage [28]. Stellate ganglion impulses cause vasospasm in pial arteries [29]. The present data further support the view that the cervical neuronal system may play a role in the control of blood flow in the cerebrovascular tree [30]. Bilateral cervical ganglionectomy results in significant vasodilatation in the basilar artery within one month [19].

Neuronal density in peripheral nerve ganglia is essential to nerve function; many types of neurotransmitters, neuromodulators and neurochemicals are produced by the peripheral nerve ganglia [31]. It has been reported that lower neuron density of the petrosal ganglion may be responsible for higher blood pressure [32]. Although the importance of cerebrovascular innervation pathways has been extensively studied, the effect of the micro-neuroanatomical architecture of the stellate ganglion on VA remodelling after BCCAL has not yet been investigated. We hypothesize that neuron density in the stellate ganglion may play a preventive role against cerebral artery elongation and dilatation secondary to BCCAL by producing vasoactive neurotransmitters. In this case, the neuron density of the stellate ganglion may be considered an important factor in the progression of subarachnoid haemorrhage. The vasospastic potency of the stellate ganglion would be diminished by decreased neuron density in stellate ganglia because vasospastic agents are synthesized in the neurons of the stellate ganglion and secreted from the nerve endings innervating the VAs. Our results imply that having fewer neurons in the stellate ganglion may cause low levels of vasospastic factor synthesis and subsequently prevent severe vasospasm of VAs after BCCAL. In conclusion, the neuron number of the stellate ganglion may play an important role in the regulation of VA volume. Ischaemic neurodegeneration of the stellate ganglion may play a preventive role against vasospasm, which returns brain circulation to normal following BCCAL.

It is critical to accurately estimate the number of living or degenerated neurons in each ganglion and basilar artery volume changes due to

vasospasm. Because previous counting methods have been biased, we have used stereological methods to estimate the number of neurons in the trigeminal ganglion and the volume values of basilar arteries [33]. Stereology is a much more effective mathematical method that relates to three-dimensional parameters, defined from the structure of two-dimensional measurements, and it can address quantitative aspects such as shape, size, number and orientation in space [12, 13]. To evaluate the severity of VA dilatation after BCCAL, the VA VDI value was the preferred measurement, instead of the radius of the lumen. The VA VDI values were estimated by assuming that the arteries were cylinders. This method estimates the volume of VAs without assuming the degree of spasmodic unaffected by overestimation errors related to neuron number in the stellate ganglion or by truncation. The method used to estimate the number of neurons in each stellate ganglion is important.

The mean VA VDI values were smaller in animals with high neuron density, and extensive VA dilatation was seen in animals with less neuron density. In our model, vasospastic molecules are synthesized by neurons in the stellate ganglion and secreted from nerve terminals that interact with the VAs. We hypothesize that low neuron density may result in a deficiency in vasospastic chemicals in sympathetic ganglia and subsequently decrease the severity of vasospasm in the VAs after BCCAL. The low neuron density of stellate ganglia may be a predisposing factor for basilar dolichoectasia and aneurysm development in steno-occlusive carotid artery diseases. We showed that high neuron density in the stellate ganglion has a beneficial effect for prevention of dangerous morphologic and histologic changes in VAs after BCCAL. Microvascular aggregation of red blood cells in the spastic cerebral arteries can trigger associated ischaemic damage in the brain. Increased cerebrovascular resistance and cerebrovascular hypertension would result in worsened ischaemia [34]. Therefore, high neuron density in the stellate ganglion may be hazardous for the brain due to blood flow-reducing effects. Thus, this effect may be particularly dangerous in diseases such as steno-occlusive carotid artery disease in which retrograde blood flow needs to be enhanced due to decreased anterior circulation.

Stellate ganglion functions on vertebral arteries

Conclusions

The neuron density of the stellate ganglion may play an important role in the regulation of VA dilatation and in the maintenance of normal cerebral circulation. Low neuron density in the stellate ganglion should be considered a risk factor in the pathogenesis of severe VA dilatation, elongation and even aneurysm development in steno-occlusive carotid artery disease. High neuron density of stellate ganglions may have a beneficial effect on acutely developed steno-occlusive carotid artery disease in the prevention of dolichoectasia, wall thinning, endothelial injury and aneurysm formation. However, it may be dangerous in its association with decreased cerebral blood flow due to required vasospastic effects for retrograde blood flow in chronic steno-occlusive carotid disease and subarachnoid haemorrhage.

Disclosure of conflict of interest

None.

Adress correspondence to: Dr. Adem Yilmaz, Department of Neurosurgery, Şişli Hamidiye Etfal Research and Education Hospital, Istanbul, Turkey. Tel: +905324266919; E-mail: ademylimaz70@yahoo.com; Dr. Mehmet Dumlu Aydin, Department of Neurosurgery, School of Medicine, Atatürk University, Erzurum, Turkey. Tel: +905323228389; E-mail: nmda11@hotmail.com

References

- [1] Oldendorf WH. Trophic changes in the arteries at the base of the rat brain in response to bilateral common carotid ligation. *J Neuropathol Exp Neurol* 1989; 48: 534-547.
- [2] Metaxa E, Tremmel M, Natarajan SK, Xian J, Paluch RA, Mandelbaum M, Siddiqui AH, Kolega J, Mocco J, Meng H. Characterization of critical hemodynamics contributing to aneurysmal remodeling at the basilar terminus in a rabbit model. *Stroke* 2010; 41: 1774-1782.
- [3] Özkan U, Aydin MD, Gündoğdu C, Onder A. Histopathologic changes in oculomotor nevre and ciliary ganglion in aneurysmatic compression injuries of oculomotor nerve. *Minim Invasive Neurosurg* 2004; 47: 107-110.
- [4] Eldawoody H, Shimizu H, Kimura N, Saito A, Nakayama T, Takahashi A, Tominaga T. Simplified experimental cerebral aneurysm model in rats: comprehensive evaluation of induced aneurysms and arterial changes in the circle of Willis. *Brain Res* 2009; 1: 159-168.
- [5] Gao L, Hoi Y, Swartz DD, Kolega J, Siddiqui A, Meng H. Nascent aneurysm formation at the basilar terminus induced by hemodynamics. *Stroke* 2008; 39: 2085-2090.
- [6] Terakawa Y, Ichinohe T, Kaneko Y. Redistribution of tissue blood after stellate ganglion block in the rabbit. *Reg Anesth Pain Med* 2009; 34: 553-556.
- [7] Aydin MD, Ozkan U, Gündoğdu C, Onder A. Protective effect of posterior cerebral circulation on carotid body ischemia. *Acta Neurochir* 2002; 144: 369-372.
- [8] Hara H, Zhang QJ, Kuroyanagi T, Kobayashi S. Parasympathetic cerebrovascular innervation: an anterograde tracing from the sphenopalatine ganglion in the rat. *Neurosurgery* 1993; 32: 822-827.
- [9] Kovacic S, Bunc G, Ravnik J. Correspondence between the time course of cerebral vasospasm and the level of cerebral dopamine-beta-hydroxylase in rabbits. *Auton Neurosci* 2006; 130: 28-31.
- [10] Suzuki N, Hardebo JE, Owman C. Origine and pathways of choline acetyl transferase-positive parasympathetic nerve fibers to the cerebral vessels in rats. *J Cereb Blood Flow Metab* 1990; 10: 399-408.
- [11] Chen XQ, Bo S, Zhong SZ. Nerves accompanying the vertebral artery and their clinical relevance. *Spine (Phila Pa 1976)* 1988; 13: 1360-1364.
- [12] Gundersen HJ, Bendtsen TF, Korbo L. Some new, simple and efficient stereological methods and their use in pathological research and diagnosis. *APMIS* 1988; 96: 379-394.
- [13] Sterio DC. The unbiased estimation of number and sizes of arbitrary particles using the disector. *J Microsc* 1984; 134: 127-136.
- [14] Hai J, Wan JF, Lin Q, Wang F, Zhang L, Li H, Chen YY, Lu Y. Cognitive dysfunction induced by chronic cerebral hypoperfusion in a rat model associated with arteriovenous malformations. *Brain Res* 2009; 1301: 80-88.
- [15] Lapi D, Marchiafava PL, Colantuoni A. Pial microvascular responses to transient bilateral common carotid artery occlusion: effects of hypertonic glycerol. *J Vasc Res* 2007; 45: 89-102.
- [16] Yang YM, Feng X, Yao ZW, Tang WJ, Liu HQ, Zhang L. Magnetic resonance angiography of carotid and cerebral arterial occlusion in rats using a clinical scanner. *J Neurosci Methods* 2008; 167: 176-183.
- [17] Yang DY, Pan HC, Chen CJ, Cheng FC, Wang YC. Effects of tissue plasminogen activator on cerebral microvessels of rats during focal cerebral ischemia and reperfusion. *Neurol Res* 2007; 29: 274-282.

Stellate ganglion functions on vertebral arteries

- [18] Falck B, Nielsen KC, Owmann CH. Adrenergic innervation of the pial circulation. *Scand J Clin Lab Invest Suppl* 1968; 102: VI: B.
- [19] Kaur G, Janik J, Isaacson LG, Callahan P. Estrogen regulation of neurotrophin expression in sympathetic neurons and vascular targets. *Brain Res* 2007; 1139: 6-14.
- [20] Bunc G, Kovacic S, Strnad S. Sympathetic nervous system exclusion following experimental subarachnoid haemorrhage prevents vasospasm in rabbits. *Klin Wochenschr* 2000; 112: 533-539.
- [21] Svendgaard NA, Göksele M, Westring S. Trigeminal nerve and brainstem catecholamine systems in cerebral vasospasm. *Neurol Med Chir* 1998; 38: 146-151.
- [22] Zhang QJ, Hara H, Kobayashi S. Distribution patterns of sensory innervation from the trigeminal ganglion to cerebral arteries in rabbits studied by wheat germ agglutinin-conjugated horseradish peroxidase anterograde tracing. *Neurosurgery* 1993; 32: 993-999.
- [23] Sindou M, Leston J, Howeydi T, Decullier E, Chapius F. Micro-vascular decompression for primary Trigeminal Neuralgia (typical or atypical). Long-term effectiveness on pain; prospective study with survival analysis in a consecutive series of 362 patients. *Acta Neurochir* 2006; 148: 1235-1245.
- [24] de SouzaFaleiros AT, de AbreuMaffei FH, de Lima Resende LA. Effects of cervical sympathectomy on vasospasm induced by meningeal haemorrhage in rabbits. *Arq Neuropsiquiatr* 2006; 64: 572-574.
- [25] Kacem K, Sercombe R. Differing influence of sympathectomy on smooth muscle cells and fibroblasts in cerebral and peripheral muscular arteries. *Auton Neurosci* 2006; 124: 38-48.
- [26] Visocchi M, Argiolas L, Meglio M, Cioni B, Basso PD, Rollo M, Cabezas D. Spinal cord stimulation and early experimental cerebral spasm: the "functional monitoring" and the "preventing effect". *Acta Neurochir (Wien)* 2001; 143: 177-185.
- [27] Visocchi M, DiRocco F, Meglio M. Protective effect of spinal cord stimulation on experimental early cerebral vasospasm. Conclusive results. *Stereotact Funct Neurosurg* 2001; 76: 269-275.
- [28] Bunc G, Kovacic S, Strnad S. The effect of sympathetic nervous system exclusion on cerebral vasospasm following subarachnoid hemorrhage in rabbits. *Acta Neurochir Suppl* 2001; 77: 107-109.
- [29] Cohen Z, Bovento G, Lacombe P, Seylaz J, MacKenzie ET, Hamel E. Cerebrovascular nerve fibers immunoreactive for tryptophan-5-hydroxylase in the rat: distribution, putative origin and comparison with sympathetic noradrenergic nerves. *Brain Res* 1992; 598: 203-214.
- [30] Amenta F, De Rossi M, Mione MC, Geppetti P. Characterization of [3H]5- hydroxytryptamine uptake within rat cerebrovascular tree. *Eur J Pharmacol* 1985; 112: 181-186.
- [31] Moskowitz MA, Renhard JF, Romero J, Melamed E, Pettibone D. Neurotransmitters and the fifth cranial nerve: Is there a relation to the headache phase of migraine? *Lancet* 1979; 8148: 883-885.
- [32] Aydin MD, Bayram E, Atalay C, Aydin N, Erdogan AR, Gundogdu C, Diyarbakirli S. The role of neuron numbers of the petrosal ganglion in the determination of blood pressure. *Minim Invasive Neurosurg* 2006; 49: 328-330.
- [33] Önder A, Serarslan Y, Aydin MD, Aydin N, Ulvi H, Kotan D, Aygül R, Gündoğdu C. The role of trigeminal ganglion neuron density in the prevention of subarachnoid hemorrhage-induced basilar artery vasospasm. *Neurosurgery Quarterly* 2009; 4: 264-469.
- [34] Ames AD, Wright RL, Kowada M, Thurston JM, Majno G. Cerebral ischemia: II-The no-reflow phenomenon. *Am J Pathol* 1968; 52: 437-453.